Preprints.org

Article

Evolution of Dew and Rain Water Resources in Gujarat (India) between 2005 and 2021

Rupal Budhbhatti , Anil Roy , Marc Muselli [*] , Daniel Beysens [*]

Article

Evolution of Dew and Rain Water Resources in Gujarat (India) between 2005 and 2021

Rupal Budhbhatti [1], Anil K. Roy [2], Marc Muselli [3,4] and Daniel Beysens [4,5,*]

[1]   National Remote Sensing Centre (Indian Space Research Organisation), Hyderabad, India.
      e-mail: rupal271@gmail.com
[2]   Dhirubhai Ambani Institute of Information and Communication Technology, 382007 Gandhinagar, India.
      e-mail: anil_roy@daiict.ac.in
[3]   Université de Corse Pasquale Paoli, Avenue du 9 septembre, BP 52, 20250 Corte, France.
      e-mail: marc.muselli@univ-corse.fr
[4]   OPUR, 2 rue Verderet, 75016 Paris, France.
[5]   Physique et Mécanique des Milieux Hétérogènes, CNRS, ESPCI Paris - PSL University, Sorbonne Université, Sorbonne Paris Cité, 10 rue Vauquelin, 75005 Paris, France. e-mail : daniel.beysens@espci.fr
[*]   Correspondence: daniel.beysens@espci.fr; ph: +33 6 89 86 47 17.

Abstract: Global warming leads in general to a reduction in precipitations and non-rainfall water contributions such as dew. The present study, carried out in Gujarat (India) for 17 years between 2005 and 2021, shows however a rare increase of the rain falls and dew condensation, the latter related to an increase in relative humidity and a decrease in wind amplitudes. Rain was obtained from meteo stations. Dew was calculated from an energy model and meteo data from 15 meteo stations (14 in India and 1 in Pakistan) and compared to early and dedicated measurements in 13 sites. Maps of dew, rain and their relative contributions during the period are provided. They show that, while rain mainly occurs during the monsoon (June to September), dew forms during the dry season (October to April). This water resource was mapped over the Gujarat state of India by using a kriging process. According to the site, the dew/rain ratios can represent between 4.6% (Ahmedabad) to 37.2% (Jamnagar) on the whole period of 17 years. This positive evolution, which is observed since 2015-2017, is likely to continue in the future.

Keywords: water resources; dew and rain increase; dew/rain ratio; dew/rain correlation; dew/rain mapping; Gujarat (India); climate change

1. Introduction

Water scarcity in the world, in the context of global warming, has been under intense discussion and debate [1]. While such discussions give new insights of sustainability, it becomes prudent to look for non-conventional water resources, particularly in arid and semi-arid regions. A recently published technical Report [2], says that one-fourth of world population is facing extreme high water stress. India ranks 13 among the 17 worst affected countries. This is also sounded by WHO's report which says that the per capita annual water availability in India has declined from 1820 cubic meters in 2001 to 1341 cubic meters and it is likely to go further down to 1140 cubic meters by 2050. Many of regions are much below the national average. The Composite Water Management Index maintained by Niti Ayog of India says that already 54% of India faces high to extreme high water stress condition which will go to water scarcity level by 2050.

Gujarat, a western part state of India, is currently reported facing extreme water stress level which may go worse in coming years (Fig. 1). Its annual rainfall is only around 600 mm with about 60 rainy days round the year. In this context, atmospheric moisture in the form of dew can potentially be harvested in a way that can offer a respite, which is commonly ignored from the water budget. Dew is naturally used by plants and small animals, particularly during droughts (see e.g., [3, 4]). In

this paper we are not considering fog because it is quite unusual in this region while dew is more commonly encountered. However, fog is undoubtedly an alternative and potential source of water in a water starved region. We are, thus, focusing only on the dew yield in the current context of global warming, whose contribution may become significant when compared to rainfall. The latter is always erratic, more so, during the dry seasons.

Large dew condensers have been experimented in Gujarat to show that the population can benefit from cost-effective fresh water [5] and even potable water [6]. In this work [6] authors mainly focused on the process of dew harvesting and its collection in one particular location in Gujarat. In our paper, we target to find out areas which have great potential of dew harvesting in the large geographical region of the whole state. It is shown that of the 12 areas where we conducted our experiment, 4 have great potential for dew collection and for using that as potable source of water in situations of dire need. We believe that such futuristic and proactive research will give a trusted information of opportunity to the local government, non-government organizations and industries for the policy framework and investment too.

Dew formation depends largely upon specific temporal climatic conditions such as clear sky, high relative humidity and low wind speed. These conditions facilitate greater radiative cooling of the earth surface and surrounding air. Along with the meteorological factors mentioned above, the dew yield also depends on the material used as condenser as well as the orientation of the condenser to collect dew. The yield can vary by at least 20% at the same location depending on the condenser's orientation with respect to the wind direction and the nearby obstacles [3, 8, 9, 10].

We are witnessing a major shift in climatic conditions globally which is attributed to the global warming. Obviously it has impact on dew formation too. Climate change may reduce the rate of precipitation. Rate of precipitation is indirectly linked with dew yield and hence most likely dew yield might decrease with global warming. A study by [4] predicts that in the Mediterranean region, dew harvesting may decline (up to 27%) by the end of the twenty first century during the dry season, however, the rate of decrease in dew yield is comparatively lesser than the projected 40% decrease in precipitation during the same period. A trend has been predicted for the North Africa area in another recent study [10]. It reports that for the century a continuous decrease of the order of −14 mm per decade is expected in rain precipitation and a clear decrease of up to 7% in the dew yields may be seen.
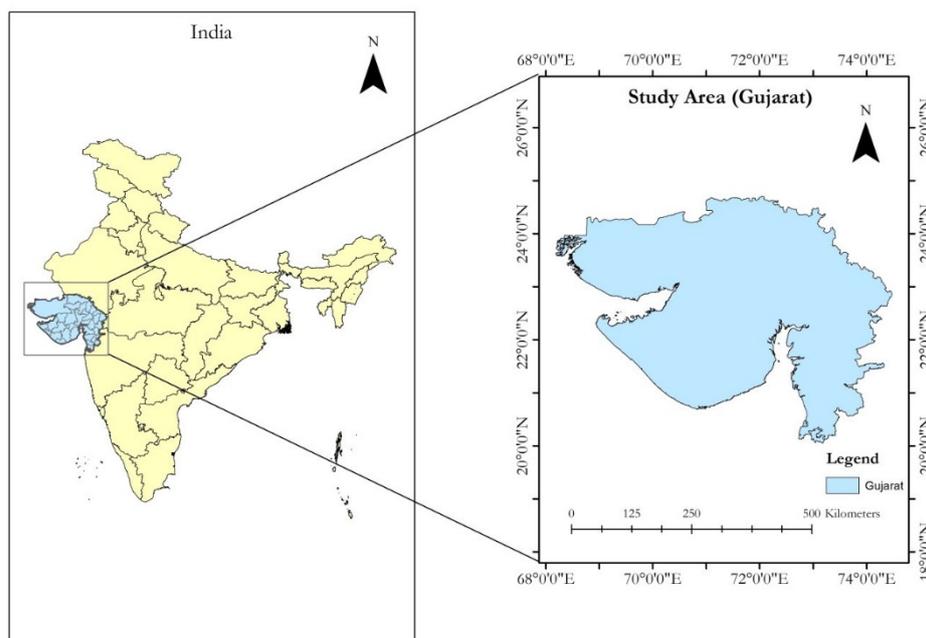

Figure 1. The Study Area of our work.

Besides [5] and [6], some more attempts have been made in the past to map the dew potential in India [11] in order to mitigate water deficiency in winter and increase soil moisture for possible agronomic exploitation. Dew was measured at 62 locations by a visual method (Duvdevani gauge, [12]) for a period of four years (1968 – 1971). More recent measurements were carried out at 6 stations in or near Gujarat [13], reported in Table 4 for winter during (2006 – 2007). In this paper it is aimed to prepare dew maps of Gujarat over a large period (17 years, from 2005 to 2021) in order to evaluate the evolution of potential of dew in this state. To compare and contrast, we also included rain potential in this region to see if the effect of global warming were similar on both the precipitation methods or it is different. To achieve this objective two things are required. One is to obtain the past years' weather data affecting the dew yield and other is to set up dew water harvesters for collecting the ground truth data and to compare it with the model prediction. If suitable condensation units similar to what reported by [5, 6] be erected at different geographical locations, regions of high yield of dew can also be identified. Authors will finally conclude with the recommendations of regions of high potential of dew so that the state government or industry houses can harvest potable water from dew for drinking purpose. This could prove to be a boon in water scarce regions in coming years.

The paper is presented as follows: Section 2 discusses meteorological data, models and the description of dew condensers used in this study. Section 3 presents krigged maps for dew and rain yields, their temporal correlation and ratio for past and recent data collected. In the Section 4 we presented our result and compared them with the past results of (1968 – 1971), (2003 – 2004) and (2006 – 2007). Comprehensive discussion is included in the Section 5. It is shown here that the monsoon plays a central role.

2. Meteorological data and Methods

2.1. Gujarat Climate

Gujarat is the fourth largest state of India in area and is located along the western coast extending between latitude 20°06′ to 24°42′ N and longitude 68°10′ to 74°28′ E. The mean elevation of Gujarat is 137 m asl. The climate of Gujarat [14] is usually characterized by a subtropical steppe climate according to the Köppen classification with an average BSh (hot, semi-arid) and locally BWh (hot, arid deserts) and BSh/Aw (Aw is tropical climate, see Tables (1 & 2). The mean of daily temperature across the year is 29.55°C. Gujarat receives a yearly mean of 589 mm of precipitation (rain), with 60.81 rainy days (16.66% of the whole year), which means that the days are usually sunny and the sky is clear during the night. It allows dew to condense. However, the mean annual rainfall over Gujarat varies widely, from 300 mm in the western part of Kutch to 2,100 mm in the southern part of Valsad and the Dangs (towards Mumbai) districts. The monsoon season extends from mid-June to September when rain happens.

The plains of Gujarat are very hot and dry. Summer is milder in coast and the hilly regions. The summer daytime temperature is around 46°C and is no lower than 34°C at night. The weather is mild and dry in winter. The average temperature during day time is 29°C and 12°C during the night. Before the monsoon, the temperatures are rising with an increased humidity in the air. It makes the dew season, when the relative humidity is high and the sky is clear, usually extending from October to April. In the following, one will thus also sometimes use the word "yearly" for dew values relative to the October – April period, unless specified.

2.2. Dew yield estimation from meteorological data

The dew resource (mm) is investigated using the Beysens energy balance model [15]. From only a few classical meteorological data, the model allows daily or hourly dew yields to be computed without adjustable parameters: Air temperature (T_a, in °C), dew point temperature (T_d, in °C), wind speed (V, in ms^{-1} , at 10 m from the ground) and cloud cover (N, in oktas). The results are shown in terms of the dew yield in mm per unit time Δt, with $\dot{h} = \Delta h/\Delta t$, where Δh, in mm, is the yield during the time period of the analyzed data and Δt is in hour. The condenser substrate is assumed planar, tilted 30° from the horizontal and thermally insulated from below. Its emissivity is assumed to be

unity (which is close to the emissivity ≈ 0.98 of a wet substrate during dew condensation, see [16]). The details of the formulation are as follows:

$$\dot{h}\left(\frac{mm}{\Delta t}\right) = \frac{\Delta t}{12}(HL + RE) \quad (1)$$

The data for $\dot{h} > 0$ correspond to condensation and $\dot{h} < 0$ to evaporation, which have to be discarded. The measurement period of the data in the present study is Δt = 0.5, 1 or 3 h., depending on the meteo stations. The quantity HL of Eq. (1) represents the convective heat losses between air and the condenser. One notes the presence of a cut-off for wind speed $V > V_0$ = 4.4 m.s^{-1} where condensation vanishes:

$$\dot{h}\left(\frac{mm}{\Delta t}\right) = \begin{cases} \left(\frac{\Delta t}{12}\right)[0.06(T_d - T_a) + RE], if\ V\ <\ V_0 \\ \quad\quad 0,\ if\ V\ \geq\ V_0 \end{cases} \quad (2)$$

The quantity RE (measured in units: mm/Δt) is related to the available radiative cooling energy, which depends on air water content (measured by T_d, in °C), site elevation H (in km) and cloud cover N (in oktas):

$$RE\left(\frac{mm}{\Delta t}\right) = 0.37\ (1 + 0.204323H - 0.0238893H^2 - (18.0132 - 1.04963H + 0.21891H^2$$
$$\times\ 10^{-3}\ T_d)\left(\frac{T_d + 273.15}{285}\right)^4\left(1 - \frac{N}{8}\right) \quad (3)$$

By filtering the data without rain or fog events and integrating the time series on a daily time-step corresponding to [$\dot{h} > 0$], the calculated daily and monthly yields and their cumulated values can be readily obtained. When comparing the calculated values with the measurements, the agreement is better than 20-30% [15, 17], the deviation being mainly due to the unavoidable local differences in air flow geometries and the presence of nearby obstacles, as discussed in the Introduction.

Table 1. Meteorological stations where dew yields were measured.

Sites	Start date	End date	Abbre-viation	Köppen Geiger climate	Lat.	Long.	Number of dew days	Sum dew (meas.; mm)	Sum dew (kriging.; mm)	Alt (m)	Distance from the sea (km)
Panandhro[1]	08/10/05	17/04/06	PH	BWh	23°40′01″N	68°46′01″E	69	11.7[8];14.2[9]	-	52	39
Kothara[2]	01/10/04	31/05/05	KO	BWh	23°13′23″N	68°45′00″E	72[3] ;74[4]	5.37[3];7.24[4]	5.74	5	21
Mithapur[5]	10/2006	05/2007	MI	BWh	22°25′30″N	69°01′26″E	89	4.03	-	4	2
Suthari[10]	01/10/05	31/05/06	-	BWh	23°02′02″N	68°54′58″E	-	4.6	3.9	37	2
DA_IICT, Gandhinagar[6]	06/12/20	31/03/21	-	BSh/Aw	23°12′23″N	72°38′51″E	95	4.3	-	76	15
DA_IICT, Gandhinagar[7]	09/12/21	31/03/21	-	BSh/Aw	23°12′23″N	72°38′51″E	55	3.62	-	76	15
Balva[6]	22/12/20	31/03/21	-	BSh/Aw	23°14′35″N	72°26′15″E	82	7.62	-	69	15
Mehsana[6]	29/12/20	31/03/21	-	BSh/Aw	23°34′08″N	72°25′12″E	19	0.88	-	90	60
Ahmadabad[6]	14/01/21	31/03/21	-	BSh/Aw	23°00′16″N	72°37′33″E	11	0.11	-	55	8
Rajkot[6]	24/01/21	26/04/21	-	BSh	22°24′57″N	70°47′17″E	86	3.47	-	113	12
Porbandar[6]	25/01/21	30/04/21	-	BSh	21°38′51″N	69°39′40″E	92	8.24	-	4	0
Junagadh[6]	24/01/21	30/04/21	-	BSh	21°30′46″N	70°27′40″E	92	1.72	-	84	30
Jamnagar[6]	25/01/21	30/04/21	-	BSh	22°31′33″N	69°59′05″E	89	11.98	-	5	8

[1] Condensing substrate is 1 m² thermally isolated OPUR foil [5]; [2] condensing substrate is 18 m² double slope non-isolated galvanized iron roof [18]; [3] roof west side; [4] roof west side; [5] [19]; [6] condensing substrate is 1 m² transparent LDPE foil (this work; see text); [7] condensing substrate is 1 m² thermally isolated black foil (this work; see text); [8] oriented east and north; [9] oriented west and south; [10] condensing substrate is 343 m² double slope oriented east and west of non-isolated galvanized iron roof [19], [20].

2.3. Direct measurements

The theoretical evaluation of Eq. [2] is compared with direct dew measurements at several locations of Gujarat for the ground truth and validation. In order to equip observers with a tool to measure dew (see section 2.5), a Do-It-Yourself kit was prepared. The kit includes all the necessary equipment for installation and measurement. A manual was prepared for easy installation. The

locations to deploy the dew collector unit were finalized by keeping the following various factors. (i) A person available at the location for taking dew readings daily in the morning. Major struggle was faced at this stage, as it is important to find a volunteer who is willing to take the readings dedicatedly daily around 6 am before sunrise (to avoid the effect of evaporation). More so, the period of collecting the ground truth fell in the peak lockdown period of the COVID pandemic. Despite this challenge the research work continued. (ii) Conveyance: Planning transportation to deploy the Dew Collector Unit at each of the location. Then the readings were recorded daily by the observer either through a phone call or on WhatsApp message. This process continued till March 2021. The dew collector units were deployed to 8 locations (Table 1), i.e., Dhirubhai Ambani Institute of Information and Communication Technology (DA-IICT, Gandhinagar), Balva, Mehsana, Ahmedabad, Rajkot, Porbandar, Junagadh, and Jamnagar.

2.4. Extraction of meteorological data

The weather stations used in this study to determine dew according to Eq. 1 for kriging correspond to international or national airports in India (14 stations) and Pakistan (one station) (Table 2). Typical meteorological parameters are systematically measured according to the standards of the World Meteorological Organization. Air temperature (T_a, °C), relative humidity (RH, %), atmospheric pressure (p, Pa) are measured in a meteorological shelter, 1.5 m from the ground. Wind speed (V, km.h^{-1}, to be transformed in m.s^{-1} in Eq. 1) and direction (sectors or degrees) are measured at 10 m from the ground. Wind speed can be extrapolated at any height z above the ground by the classical logarithmic variation (see e.g. [21]):

$$V_z = V_{10} \frac{ln(z/z_c)}{ln(10/z_c)} \quad (4)$$

where V_{10} is wind speed at 10 m and z_c is the roughness length where $V = 0$ (generally $z_c = 0.1$ m in flat areas like airports). Available data on 15 sites were extracted from the online database Weather Underground (WU) [22] during the period 2005-2021 (Table 2). One notes that dew does not form before and during the monsoon, cloudy season (June to September). The results presented in this article will therefore correspond to only the non-cloudy period, from October to April, unless specified. In order to assess the results of the kriging methods, we also worked with a network of ground stations where daily dew yields were measured before sunrise at 6 am (section 2.3, Table 1).

It has to be noted that some measurement sites do not present cloud cover measurements after 2014. For those stations, a dedicated study was made in section 3.1 to validate the use of a mean cloud cover ($N = 1$) for those missing data.

Table 2. Meteorological sites (15 airports: 14 in India and 1 in Pakistan) where atmospheric data are collected with typical climate and distances from the sea. The time steps in h. of collected data are also reported.

Country	Sites	Period of data	Abbrev.	Köppen Geiger climate	Dew (D) and/or Rain (R)	Lat.	Long.	Alt (m)	Data Dew time step (h)	Distance from the sea (km)
India	Ahmadabad	2005-2021	AH	BSh/Aw	D / R	23°04′38″N	72°38′05″E	58	0.5-1	83
India	Bhuj[1]	2005-2021	BH	BSh	D / R	23°17′16″N	69°40′13″E	82	3	47
India	Vadodara	2005-2021	VA	BSh/Aw	D / R	22°19′46″N	73°13′10″E	39	0.5-1	25
India	Bhavnagar[1]	2005-2021	BV	BSh	D / R	21°45′08″N	72°11′07″E	13	3	12
India	Daman[1]	2005-2021	DA	Aw	D / R	20°26′04″N	72°50′36″E	10	3	2
India	Jamnagar[1]	2005-2021	JA	BSh	D / R	22°27′56″N	70°00′45″E	21	3	10
India	Kandla[1]	2005-2021	KA	BWh	D / R	23°06′46″N	70°06′01″E	29	3	2
India	Junagadh[1]	2005-2021	JU	BSh	D / R	21°19′01″N	70°16′13″E	51	3	59
India	Porbandar[1]	2005-2021	PO	BSh	D / R	21°38′55″N	69°39′26″E	5	3	1
India	Rajkot[1]	2005-2021	RA	BSh	D / R	22°18′33″N	70°46′46″E	135	3	71
India	Surat[1]	2005-2021	SU	Aw	D / R	21°7′3.6″N	72°44′43″E	5	3	17
Pakistan	Karachi	2005-2021	KR	BWh	D / R[2]	24°54′24″N	67°09′39″E	21	0.5	10
India	New Delhi	2005-2021	NE	BSh	D / R[2]	28°33′00″N	77°05′00″E	220	0.5	925
India	Jaipur	2005-2021	JP	BSh	D / R[2]	26°49′27″N	75°48′44″E	385	0.5-1	794
India	Gwalior[1]	2005-2021	GW	Csa	D / R[2]	26°17′36″N	78°13′40″E	188	0.5-3	709

[1] Cloudy sky conditions data from [22] missing on 2014-2021 (replaced by $N = 1$, see text); [2] Rainfall data are extracted from ERA5/ECMWF Copernicus database [23].

Dew yields were computed from Eqs. 1-4 with time period $\Delta t = 0.5, 1, 3$ h. depending upon the sites. The wind directions are computed from the sectors (N, NNE, NE, E, ESE, SE, S, etc.) by using a standard law of proportionality: 0° for north, 180° for south. Cloud cover in oktas was computed from the observation of sky cover using the correspondence from national weather service glossary [24]: CLR (Clear): $N = 0$; FEW (Few): $N = 1$; SCT(Scattered): $N = 3$; BKN (Broken): $N = 5$; OVC (Overcast): $N = 8$. The rainfall data, available on a daily time-step, are extracted from National Data Centre, Pune for 11 cities including the stations of Gujarat reported in Table 1, whose meteo data are also used for the stations noted in Table 1. For Karachi, New Delhi, Jaipur and Gwalior, rainfall data (2005-2021) are extracted from the ERA5/ECMWF model [23] using the historical land monthly averaged database from 1950 to present (see Table 2). The study period is from 2005 to 2021.

2.5. Dew Measurements

A number of dew measurements have been carried out on planar condensers (Fig. 2). The dew condenser is composed in three different parts.

Firstly, the surface area of the condensing panel is of 11 m² . It is inclined at 30° angle from horizontal. The study by [25] shows that an angle near 30° is the optimal inclination as this minimizes the heat exchange effect caused by wind, while allowing water to be recovered by gravity. The panel includes the following parts: Condenser sheet, Styrofoam and cardboard sheet. Condenser sheet is the most important part of the entire dew collector unit. Dew condenses based on the radiative cooling property of the condenser and water drops slide down due to its wetting properties. Two different materials were used based on their availability in the market: One is transparent Polyethylene Sheet and the other is UV stabilized black LDPE foil. Both were kept at DA-IICT ground to check their yield. The black foil has larger radiative cooling and hence a somewhat higher dew yield compared to transparent Polyethylene sheet, due mainly to its higher emissivity (~ 0.98 [26]) versus ~ 0.87 [3]. The emissivity difference matters only during the early times of condensation when the surface is mostly dry; later surfaces are wet and exhibit the same emissivity close to that of water (0.98) [16].

The condenser is wrapped over a Styrofoam sheet for insulation. Single Styrofoam sheet of 1 m × 1 m is not available in the market, hence we had to go for two 0.5 m × 1m sheets and join them using adhesive. The cardboard sheet is used merely as a support over which the Styrofoam sheets can be used. The main advantage of using cardboard sheet is that it is not costly, easily available and has light weight. What observed in this is that the dew water seeps from the hole made for zip ties (used for connecting panel with the supporting frame), making the cardboard sheet wet. So, this could reduce the durability hence we tried to other variations such as plywood sheet, PVC sheet and green fiber sheet. However, all of these are good in terms of durability but has their own disadvantages in terms of unnecessary increased in the cost of collector unit and higher weight. Hence cardboard sheet was finalized. Light weight frame structure was made using easily available low-cost PVC pipe material of 2.5 cm diameter.

Finally, the condensed dew water drops slide down by gravitation to the provided drain channel (as shown in Fig. 2). The drain channel was made of galvanized iron material. In our initial phase of prototype development, we used it as it is. But over the time we found that it has corrosion problem, which makes the surface rough and hence creating hindrance to the flow. We decided to paint it to prevent the corrosion. The drain channel was designed with a slope on the other end so that dew water drops which came to this channel from the condenser surface ultimately got collected in a 250 ml bottle at that end. The cap of this bottle was fixed in a leak-free way at this end of the drain channel using an adhesive so that the bottle could be screwed easily in that cap and store the dew water in night. The bottle, later in the morning, could be unscrewed to remove from the frame for taking the measurement of the daily yield.
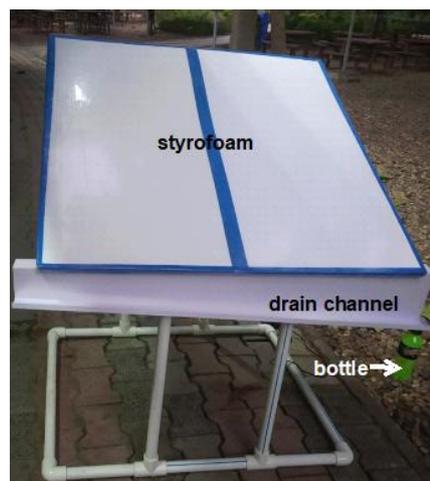

Figure 2. The DIY dew condenser unit (with transparent polyethylene sheet).

2.6. Kriging maps

Kriging is a method of spatial interpolation. It allows the value of a parameter data at non-sampled sites to be predicted by using the spatial correlation between sampled points to interpolate the values in the spatial field. The interpolation is based on the spatial arrangement of the empirical observations and does not refer to a supposed model of spatial distribution. The method presumes that a spatial correlation exists with the distance or direction between the sample points. The kriging weights are calculated in such a way that points close to the location of interest have more weight than those farther away. The kriging predictor relates a mathematical function to all or certain determined points, located within a specific radius and defines the value for each location. The interpolated data are calculated at a specific location from a general formula consisting in a weighed sum of the data [27]:

$$\hat{Z}(s_0) = \sum_{i=1}^{P} \lambda_i Z(s_i) \qquad (5)$$

Here $Z(s_i)$ is the measured value at the ith location, s_o is the predicted location, p is the number of measured data and λ_i is a weighing coefficient to determine and relate to the ith location. The weighing

8

coefficients are not only built on the distance between the sampling points and the projection location, but also on the spatial organization of the sampling points. The spatial autocorrelation is quantified in order to consider the spatial arrangement in the weighing, making to depend on the distance from the estimate location and the spatial interactions between the values documented around it. A semi-variogram can thus be estimated from point pairs:

$$\hat{\gamma}(h) = \frac{1}{2n(h)} \sum_{i=1}^{n(h)} [Z(s_i) - Z(s_i + h)]^2 \qquad (6)$$

Where

$$n(h) = Card\{(s_i, s_j)/|s_i - s_j| \approx h\} \quad (7)$$

Here *Card* represents the number of elements for the given condition. The projected semi-variograms are fitted by a spherical model already proposed for rainfall spatial estimation [28-31]. When the coordinates of the ground measured stations (e.g. Kothara or Panandhro) do not correspond exactly to a kriging point, we have considered the nearest grid point to determine the estimated values.

3. Dew results.

This section is organized as follows. One will first present the maps of the important meteo data for dew formation, with a special study concerning cloud covers whose values are unfortunately missing in several sites after 2014. One will see that replacing those missing values by a mean value $N = 1$ is justified. Then one will present the dew maps and their evolution in the period 2005 – 2021 and compare the values with already existing data, including our own measurements.

3.1. Significant meteo data

As seen in section 2.2, the important meteo data that control dew formation are the cloud cover N, windspeed V and the difference T_d - T_a between the dew point temperature and air temperatures. Relative humidity RH is nearly proportional to T_d-T_a at constant T_a, with a coefficient that however changes only smoothly with T_a [3].

Concerning the cloud cover, several measurement sites do not have cloud cover measurements after 2014. One thus separated our study in two sub-periods: 2005-2013 and 2014-2021. For all meteorological airports, the dew yields h was calculated and mapped (Fig. 3) from Eqs 1-2 using either the measured cloud cover (N_{meas}) or a constant value (N = 0, 1, 1.5, 1.7). Table 3 also presents the statistical coefficients of the study. On 2005-2013, similar statistical parameters are observed with N_{meas} (mean: 3.4 ± 2.3 mm; min/max: 0.7/8.4 mm; median: 2.1 mm) or $N = 1$ (mean: 3.4 ± 2.5 mm; min/max: 1/10.4 mm; median: 2.5 mm). The observed differences remain within the uncertainty of the physical model [16].

The mean ratio for the period 2005-2013, $\epsilon(N) = \overline{(h_N/h_{N_{meas}})}$ experiences the following results: $\overline{\epsilon(0)}$ = 1.40 ± 0.19; $\overline{\epsilon(1)}$ = 0.99 ± 0.18; $\overline{\epsilon(1.5)}$ = 0.83 ± 0.18; $\overline{\epsilon(1.7)}$ = 0.76 ± 0.17. The best comparison is obtained for $N = 1.0$, as seen in the maps of Fig. 3. It leads to the conclusion that, in the period 2005-2013, the krigged map with $N= 1$ well corresponds to the map calculated with N_{meas}. One will thus consider in the following calculations for the period 2014-2021 the mean value $N = 1$ when this parameter is lacking.

Table 3. Mean yearly dew yields (mm.yr^{-1}) on studied sites (see Tables 1 & 2) for the same periods (October to April): 2005-2013 with N_{meas} and $N = 1$ (imposed) and 2014-2021 with $N = 1$ (imposed).

Oct-Apr	2005-2013 (N_{meas})	2005-2013 ($N = 1$)	2014-2021 (misssing data N	2005-2021 (missing data N

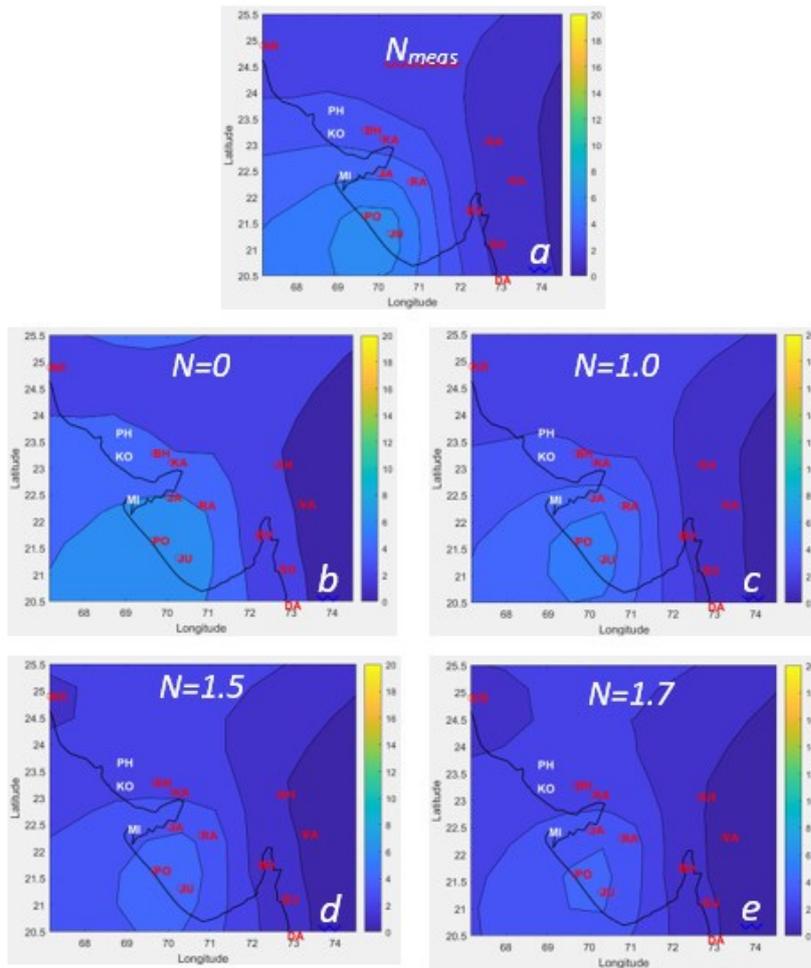| min	0.	1.	2.	2.
max	7	0	1	1
mea	8.	10.	18.	12.
n	4	4	0	2
sdt.	3.	3.	5.	4.

Figure 3. Comparison of mean yearly dew yields (mm.yr^{-1}) in the period 2005-2013 as calculated with the measured cloud covers (a) and assuming constant cloud cover values $N = 0$ (b), 1.0 (c), 1.5 (d), 1.7 (e). The letters refer to the stations (see Tables 1 and 2).

Figure 4 reports the krigged meteorological conditions during the dew condensation periods corresponding to, respectively, RH, the difference T_d - T_a between the dew point temperature, and windspeed V at 10 m from the ground. One sees that, as expected, the RH and T_d - T_a maps are quite similar, with increase (RH) or decrease ($T_d – T_a$) towards west. Windspeed decreases towards SSE.
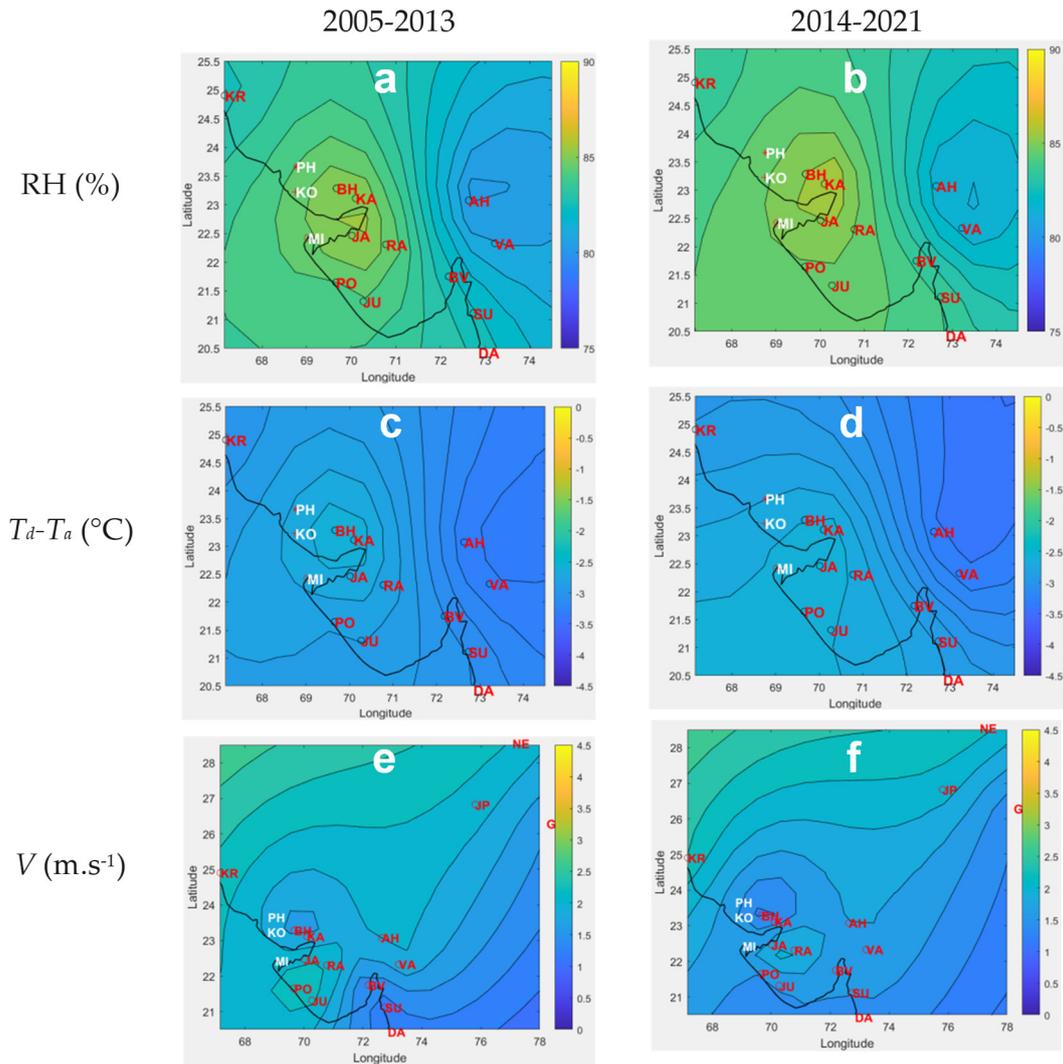
Figure 4. Krigged map (zoomed on the Gujarat area) during dew condensation for (a, b, c): $T_d - T_a$ (°C); (d, e, f): V (ms^{-1}); (g, h, i): RH (%) values. For 2005-2013 (N_{meas}, a, d, g), 2005-2013 ($N = 1$ imposed, b, e, h) and 2014-2021 ($N = 1$ imposed, c, f, i). Marks: Black circles: meteorological airport stations for kriging; "*", "+" and "o" respectively Panandhro (PH), Kothara (KO) and Mithapur (MI) sites (where dew yields are measured). The other letters refer to the stations (see Tables 1 & 2).

3.2. Dew maps

One separates the study in two periods starting from 2005: 2005-2013 and 2005-2021. The calculations for 2005-2013 are based on the observed cloud cover at the weather stations extracted from [22]. For 2014-2021, the mean value $N = 1$ was imposed when missing (see section 3.1). The maps are shown in Fig. 5; they are quite similar with a rise in the whole period 2005-2021 with respect to the period 2005-2013, as also observed in Table 3 where the statistical coefficients are reported. This evolution is analyzed in details in the following section 3.3.

Concerning the spatial distribution of dew, one observes an increase towards SSW for both periods as a result of increasing RH towards west and decreasing windspeed towards SSE (Fig. 4). One also notes a dew rise towards NE, due to the weight in the kriging of New Delhi, which exhibits a high dew potential as well as Jaipur.
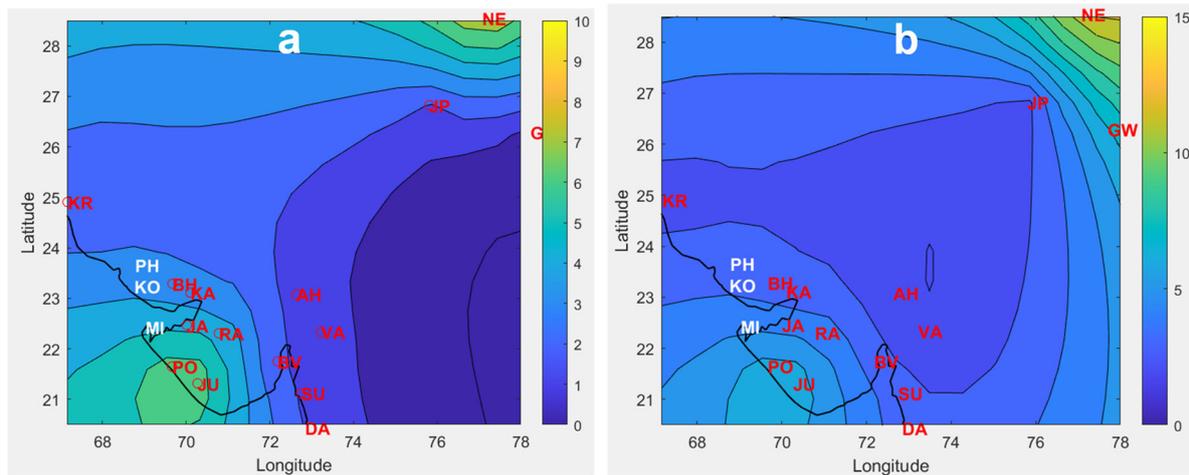
Figure 5. Krigged map for yearly dew yields (mm). (a) 2005-2013 with N_{meas}; (b) 2005-2021 with $N = 1$ for missing data. Marks: Black circles: meteorological airport stations for kriging; Panandhro (PH), Kothara (KO) and Mithapur (MI) sites (measured dew yields).

3.3. Dew evolution

In Table 3 are shown the dew yield statistics for two periods, 2005-2013, 2014-2021 and the entire period 2005-2021. It is seen a rise in the mean values, from 3.4 mm.yr^{-1} between (2005-2013) to 5.8 mm.yr^{-1} (2014-2021), with 4.6 mm.yr^{-1} for the whole period (2005-2021). This rise corresponds to Fig. 5 maps and is more evidently displayed in Fig. 6 where the evolution between 2005 and 2021 is directly reported.   The increase in dew yield is related to the corresponding (weak) increase of the relative humidity (Figs. 4ab) (2005-2013: Mean RH = 83.6%; 2014-2021: Mean RH = 84.4%) and the (slight) decrease in the wind regime (Figs. 4ef) (2005-2013: Mean V = 1.9 m/s; 2014-2021: Mean V = 1.7 m/s).

The increase in dew is nevertheless heterogeneous when looking at Fig. 6. With the exception of the city of Jaipur where the increase is limited to about 2 mm, the areas of New Delhi and Gwalior show a stronger increase in dew yields (more than 15 mm over the period). These regions are already showing high dew yields, see Fig. 5, which will be then reinforced. In the southern part of the region, coastal sites such as Daman, Surat and Bhavnagar exhibit yield increases of 5-8 mm over the period. The least advantaged micro-region remains the west coast and the northern part of Gujarat state (from Panandhro to Rajkot), where the increase is limited to a few mm. These regions, however, exhibit the largest yields of the area (see Fig. 5). The main changes are thus observed on the axis SSW to NE when only a weak increase is found for Gujarat regions such as near Porbandar and Junagadh, and a neat increase at the NE of the domain, near New Delhi.
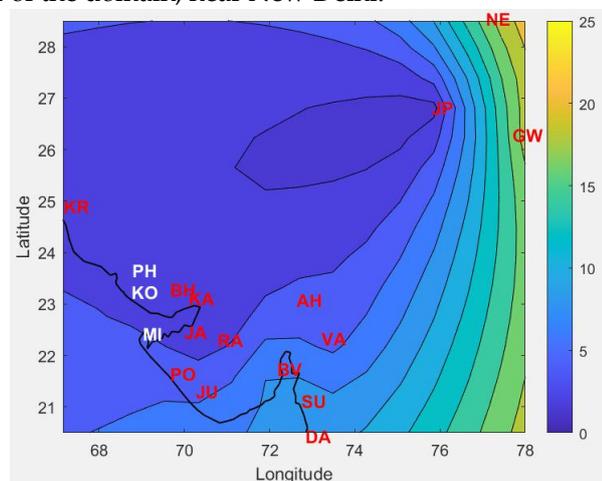

Figure 6. Dew yields evolution (mm) between 2005 and 2021 (N_{meas} if available and $N = 1$ on 2014-2021 whenever cloud cover are missing).

3.4. Comparison with direct measurements

3.4.1. 1969-1970 data

Raman et al. [11] developed from October 1968, a network of 62 sites to measure dew yields all over India. The method was visual (Duvdevani gauge [12]). A dew map was drawn concerning the dew season October 1969 – March 1970. The region of Gujarat is shown in Fig. 7a and compared to our data in Fig. 7b for the same period correspondding approximately to the dew season October 2005 - March 2006. Although our study is 26 years later, the repartition is similar, with the largest yields on S-SW (coastal area) and NE.

Four stations in [11] also appear in our database: New Delhi, Surat, Vadodara (Baroda) and Rajkot. For years 1969 and 1970, dew deposition (mm) averaged at these sites were measured between October and March. Figure 5c compares the mean measured monthly dew yields (mm) versus the mean estimated monthly dew yield obtained in our study between 2005 and 2013. Even though the periods are different, modeled and measured data are in reasonable agreement as shown by the ratio of summed values sum(h_{calc}) / sum(h_{meas}) = 0.78 (R² = 0.79).
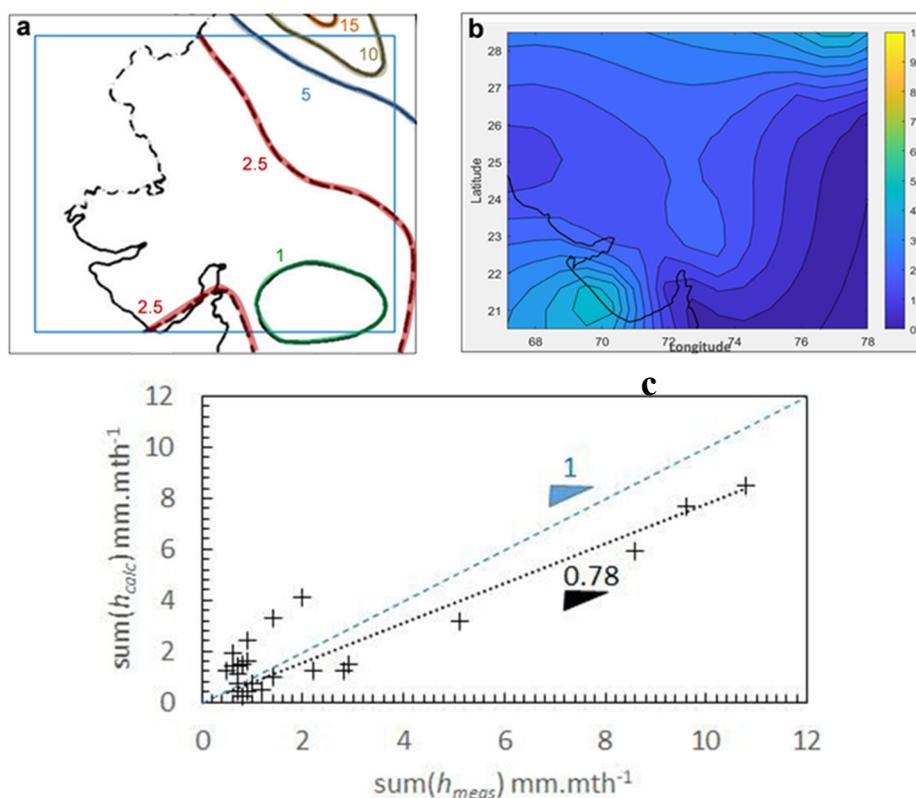

Figure 7. Cumulative dew yields (mm) in the Gujarat area between October and March. (a): Map adapted from [11] (1969-1970 dew season); (b): Map in the same period (2005-2006) (this study). (c): Cumulative dew yields (mm.mth⁻¹) averaged on the dew seasons between 2005 and 2013 (this study) and from the averaged values of New Delhi, Surat, Vadodara/Baroda, Rajkot during the same period 1969-1970 (data from [11]).

3.4.2. 2005-2006 and 2006-2007 data

The experiments reported below have been carried out between October and May. The May data being found always negligible, the cumulative yields during the period OcT-May will be thus compared to the calculation performed on the period Oct. – Apriol.

Between October 2004 and May 2005, Sharan et al. [18] studied dew events and dew yields on a galvanized roof. The condensing device was composed of two inclined surfaces (total 18 m²) in Kothara (see Table 1). With about 70 dew days, cumulative measured dew yields represented respectively 5.4 mm and 7.2 mm for east and west sides of a non-thermally isolated, steel roof (Tables

1 & 2). Corrections for thermal isolation and use of radiative foil is expected to give a factor of 1.4 [18], corresponding to 7.5 mm (east side) and 10.1 mm (west side). According to the physical model Eq. 1 (1 m², 30° tilt angle, thermally isolated) and the local meteo data, the expected yield was estimated to be 15 mm for the period [5], a value somewhat larger than the measurements but still in the uncertainties of both the model and the measurements.

During the same period (Fig. SI-1), the dew yield estimated at the closest grid point from the measurement site (11.1 km distance) is 5.7 mm. Hence, the value estimated by kriging lies between the measurement of east and west sides roofs without thermal isolation (5.4 mm and 7.2 mm). The mean meteorological conditions for dew deposition observed in Kothara between October 1, 2004 and May 31, 2005 are $\bar{V}$ = 2.23 ± 1.59 m.s^{-1}, $\overline{RH}$ = 91.8 ± 7.9 % and $\overline{T_d} - \overline{T_a}$ = -1.46 ± 1.55 °C. According to kriging, between October 2004 to May 2005, the mean values are $\bar{V}$ = 2.1 m.s^{-1}, $\overline{RH}$ = 85.6 % and $\overline{T_d} - \overline{T_a}$ = -2.53 °C. All values are in fair agreement with the mean measured values.

A roof used as condenser system (343 m²) was also studied during the period Oct. 2005 – May 2006 at Suthari, 12 km from the above site of Kothara [19, 20]. The condensing surface was galvanized iron plates for dew harvesting. The roof presented one slope facing W and the other E with a tilt angle of 15° and was not thermally isolated. The dew yields during the period was 4 mm (5.6 mm rescaled with temperature isolation). The corresponding kriging map in the same period (Fig. SI-2) concludes to a close value of 3.9 mm per year for the nearest grid point, 35 km south from Suthari, in relatively good agreement with the measured values.

Between Oct. 2006 and May, 2007, measurements carried out at Mithapur (Table 1) gave 4.0 mm in total. The kriging process on the same period leads to 3.2 mm. One sees that the measured and calculated Kriging values, although somewhat smaller, agree relatively well within the uncertainties that can go up to 30% in the model [15], due mainly to the different air flow configurations between model and experiments.

3.4.3. Other past data

Other unpublished data have been also reported by G. Sharan [13] in different cities during the dry, dew season (Oct. 2006 – Apr. 2007). Table 3 summarizes the results and Figure 8 compares with the mean of calculated data during each month of the dry season October to April between 2005 and 2013.

Table 4. Comparison between Sharan's dew measurements (Oct. 2006 - April 2007 [13]) and this study (calculated dew averaged between 2005 and 2013), expressed in mm.

| Site		Oct.	Nov.	Dec.	Jan.	Feb.	March	April	Sum
New Delhi	Sharan	1.17	2.02	2.73	2.32	1.38	0.56	0.07	10.25
	Our Study	0.46	0.76	1.93	2.67	1.76	0.79	0.10	8.47
Vadodara	Sharan	0.84	0.51	0.13	0.08	0.12	0.07	0.05	1.79
	Our Study	0.34	0.29	0.41	0.26	0.11	0.03	0.06	1.50
Surat	Sharan	1.82	1.01	0.83	1.28	0.97	1.54	0.73	8.19
	Our Study	0.13	0.17	0.29	0.29	0.16	0.26	0.60	1.90
Junagadh	Sharan	0.70	0.57	0.13	0.36	0.34	0.20	0.11	2.42
	Our Study	0.99	0.40	0.33	0.42	1.05	1.74	1.88	6.81
Rajkot	Sharan	1.13	0.52	0.16	0.37	0.55	0.43	0.19	3.37
	Our Study	1.21	0.26	0.58	0.50	0.89	0.83	0.74	5.01
Bhuj	Sharan	1.62	0.99	0.67	0.63	0.82	0.90	1.37	6.99
	Our Study	0.47	0.10	0.18	0.25	0.56	0.90	0.95	3.41
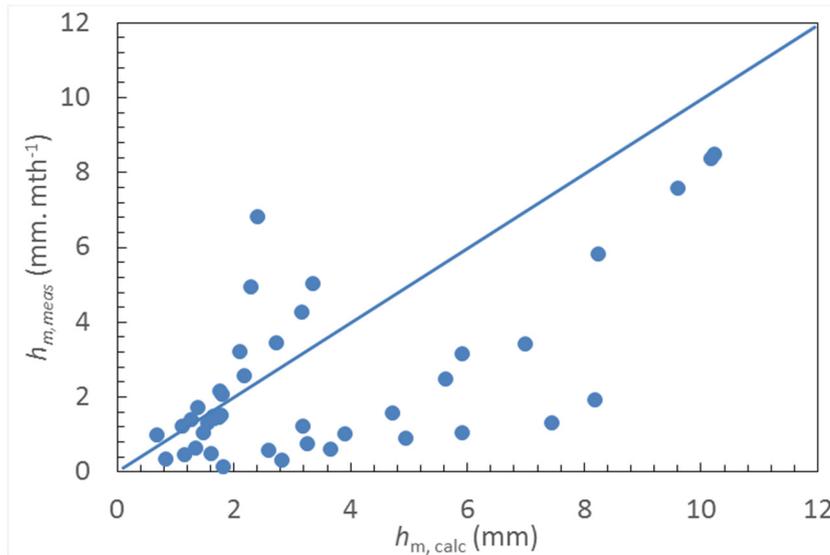
Figure 8. Correlation between the monthly measured dew yields (in mm.mth^{-1}) from Sharan's database (Table 3) and this study, concerning the mean between 2005-2013 of each month of the dry, dew season (October to April, Table 3).

3.4.4. Present measurements

Between December 06, 2020 and April 30, 2021, dew condensers were implemented on 9 sites (see Table 1). The data are compared with a calculation using (i) a daily dew yields h_{dew} (mm.day^{-1}) and (ii) a number of dewy days t_{dew} (in % of total investigated days) using the physical model Eq.1 with time step (Δt = 12h) and assuming N = 1 when the value was missing (see section 3.1). The monthly (30 days) means are calculated as:

$$\bar{h} = 30 \times \frac{\Sigma(h_{dew})}{p} \quad (8)$$

and

$$\bar{t} = 30 \times \frac{\Sigma(t_{dew})}{p} \quad (9)$$

Here p represents the number of days for each studied site, which are different according to the measured and calculated sites. The comparison between estimated (model) and measured dew yields (mm.mth^{-1}) and dewy days (%) are plotted on Figs. 9 and 10.

For the 9 sites studied, the average monthly yields ranged from 0.043 to 3.782 mm.mth^{-1} (average = 1.454 mm.mth^{-1}). The Balva and Gandhinagar sites (monthly mean 2.3 mm.mth^{-1} , 83% of dewy days, OPUR white foil substrate) shows the highest correlation with estimates obtained from Ahmedabad airport (1.8 mm.mth^{-1} , 80% of dewy days, WU database). The other sites show fair correlations (Porbandar, measured 2.6 mm.mth^{-1} vs 1.8 mm.mth^{-1} estimated). Some sites (Junagadh) overestimate the dew production (1.8 mm.mth^{-1} measured vs 0.5 mm.mth^{-1} calculated) and others like Jamnagar underestimate this production (3.7 mm.mth^{-1} measured vs 0.5 mm.mth^{-1} estimated). The main reason for these differences is the estimated number of dew days, lower than the actual measurement, e.g., for Rajkot, Porbandar, Junagadh and Jamnagar the measured dew day percentages are between 93 and 97% when the model estimates these rates between 42 and 70%. This difference is mainly due to the fact that meteo data are not taken at the measurement site itself. Local variations of e.g., RH and air flows can lead to substantial variations in the measured dew yield.
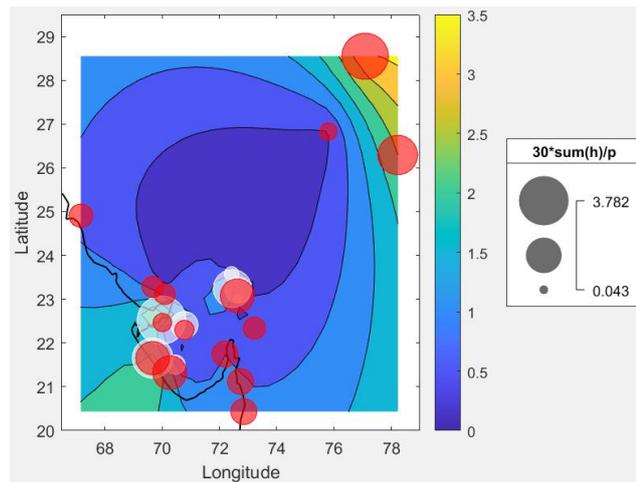
Figure 9. Monthly dew mean (Eq. 8; in mm.mth^{-1}) for measured (white circles) and calculated (red circles) sites during the same time period. Mapping data are obtained by the kriging process using the WU database.
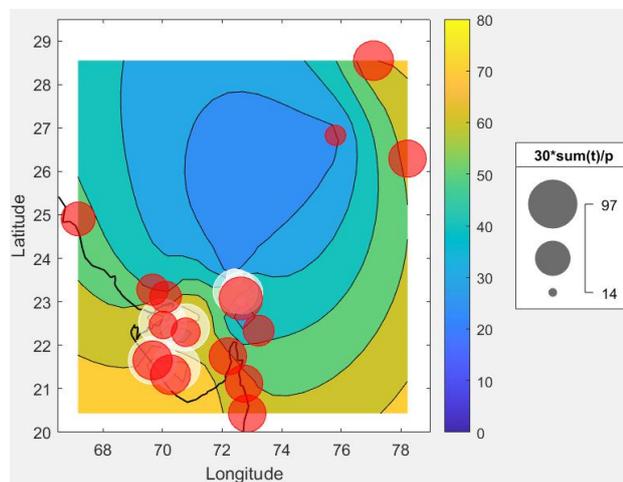

Figure 10. Monthly dew days mean (Eq. 9; in %) for measured (white bubbles) and calculated (red bubbles) sites. Mapping data are obtained by the kriging process using WU database.

4. Rain results

Except for a few cities where rainfall data are extracted from the ERA Copernicus database [23] (see Table 2), rain yields (mm) data were obtained from the Indian national meteorological network National Data Centre, Pune, on a daily time-step. These data are integrated on monthly and yearly bases (mm.mth^{-1}, mm.yr^{-1}) in order to compare with dew yields.

Figure 11a describes the rainfall profile for the Gujarat district during the dry season (October to April). Here we find a decreasing axis of rainfall between the NE and SSW of the region. The coastal area of the Arabian Sea are poorly supplied with rain, with less than 50 mm.yr^{-1}, while cities located further from the coast such as New Delhi or Jaipur benefit from rainfall amounts that can reach 100 or even 150 mm.yr^{-1}. The evolution of rainfall between 2005 and 2021 (Fig. 11b) shows an average increase during the dry season. One notes an area around Ahmadabad where the amount of rainfall has not changed. Moving away by concentric circles from this area, the measurements show an increase in rainfall in the 15 years period with variations that can reach 100 mm specifically in the coastal regions of Junagadh, Surat and Daman but also inland, near New Delhi.
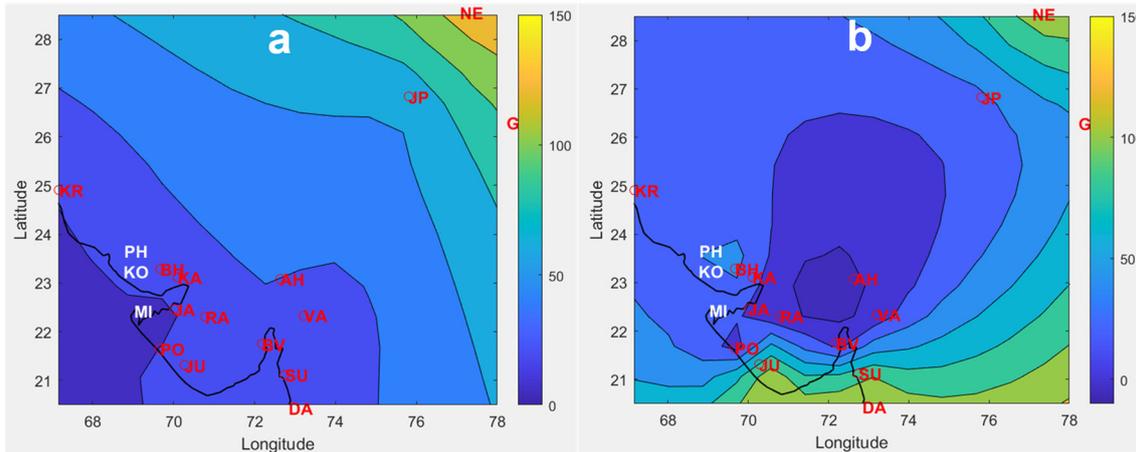
Figure 11. (a): Mean yearly rainfall (mm) on 2005-2021 (October -April, with zoom on the Gujarat area). (b): Variation of yearly rainfall (mm) between 2021 and 2005 (October –April, with zoom on the Gujarat area).

5. Dew - rain correlations

5.1. Correlation in dew and rain evolutions

One shows in Fig. 12 the cumulative dew and rainfall evolutions. The choice of cumulative values smooth the scattering of data and makes the trends more visible. One thus observes in Fig. 14 that dew and rain obeys in general similar behavior. One notes a near constant rise between 2005 and 2017 and an acceleration later, from 2018 to 2021.

Concerning dew, a good example is New Delhi where the mean dew rate between 2005 and 2017 was 1.44 mm.mth^{-1} and from 2018 to 2021, 2.44 mm.mth^{-1}. There are some exceptions, like Rajkot, where the acceleration is not observed, with the mean dew rate 2005-2017 is 0.71 mm.mth^{-1} and the mean dew rate 2018-2021 is 0.57 mm.mth^{-1}. On 2005-2017, the monthly rates vary from 0.25 mm.mth^{-1} (Ahmedabad) to 1.44 mm.mth^{-1} (New Delhi); mean = 0.54 mm.mth^{-1}. The acceleration during the recent years (2018-2021) can be considered as moderate on sites like e.g. Ahmedabad- Vadodara (0.25 to 0.49 mm.mth^{-1}), Bhuj ($N = 1$ assumed, 0.44 to 0.64 mth^{-1}), Kandla ($N = 1$ assumed, 0.46 to 0.61 mm.mth^{-1}) or Karachi (0.32 to 0.48 mm.mth^{-1}). It is much more obvious on sites like New Delhi (1.44 to 2.44 mm.mth^{-1}), Gwalior ($N = 1$, 0.45 to 3.11 mm.mth^{-1}), Surat - Bhavnagar ($N = 1$, 0.33 to 1 mm.mth^{-1}).

Concerning rain, the general trend is the same as dew. While most sites behave as dew, with an acceleration after 2015 - 2017, some sites remain stable (Rajkot, Gwalior). One notes that some sites undergo a decrease in rainfall from 2015 such as Karachi, Porbandar, Vadodara and Ahmedabad.
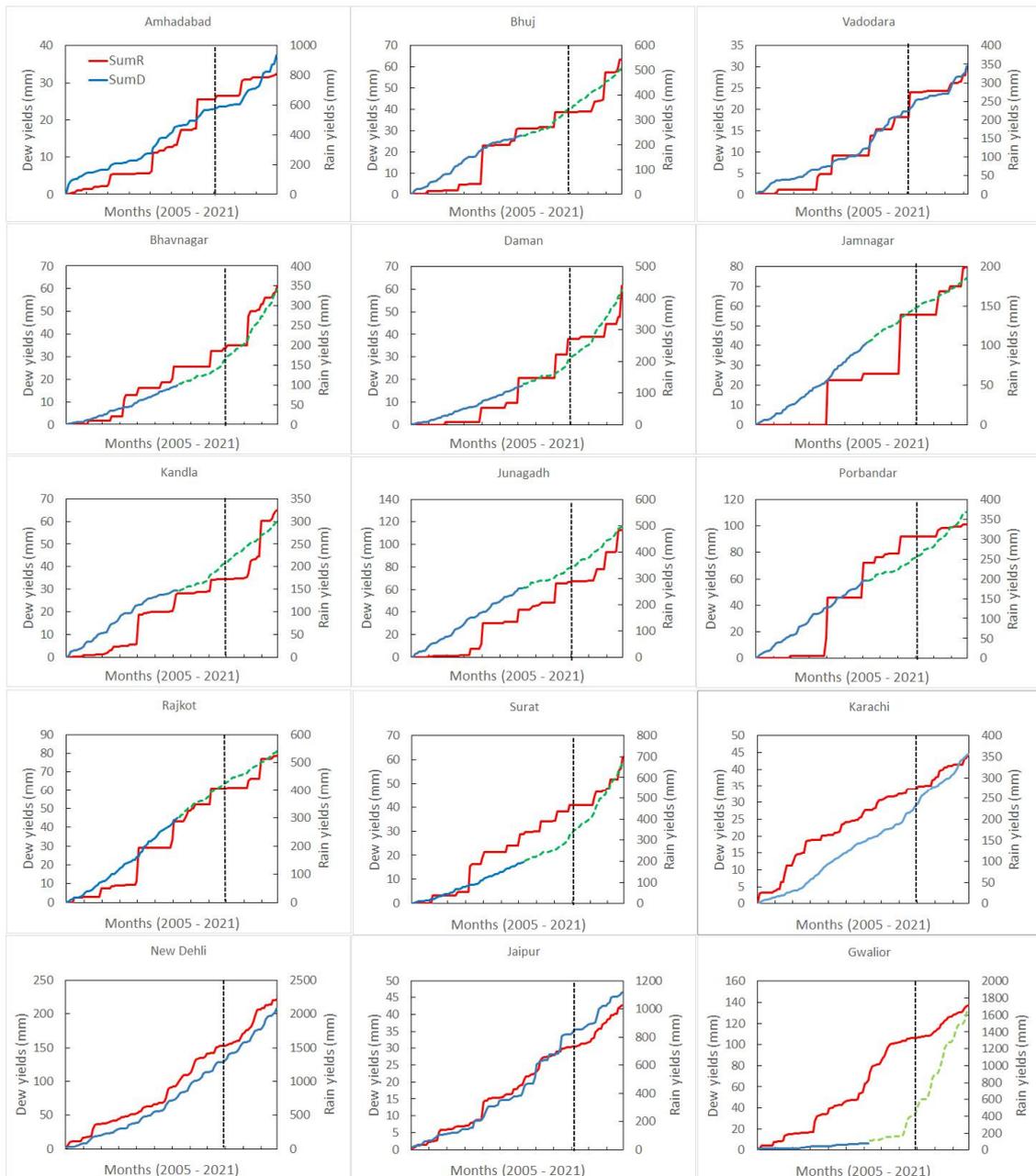
17

Figure 12. Evolution of the summed values sum(h_{dew}) (dew, full blue line for N_{meas} and interrupted green line for imposed $N = 1$) and sum(h_{rain}) (rain, mm, full red line) for the studied sites. The unit of dew and rain (ordinate) is mm. The abscissa is month, from 2005 to 2021.

5.2. Ratio of dew and rain contributions

The contribution of dew to the water balance is measured by the ratio of summed dew and rain values during the dry seasons of the period. Figure 14 presents the mean ratios at the different sites. The ratio varies between 4.5% (Jaipur) or 4.6% (Ahmedabad) to 37.2% (Jamnagar) or 32.8% (Porbandar). The high ratios combine large dew and low rain and correspond to coastal sites while, in contrast, the low ratios correspond to low dew and high rain and are more inland.
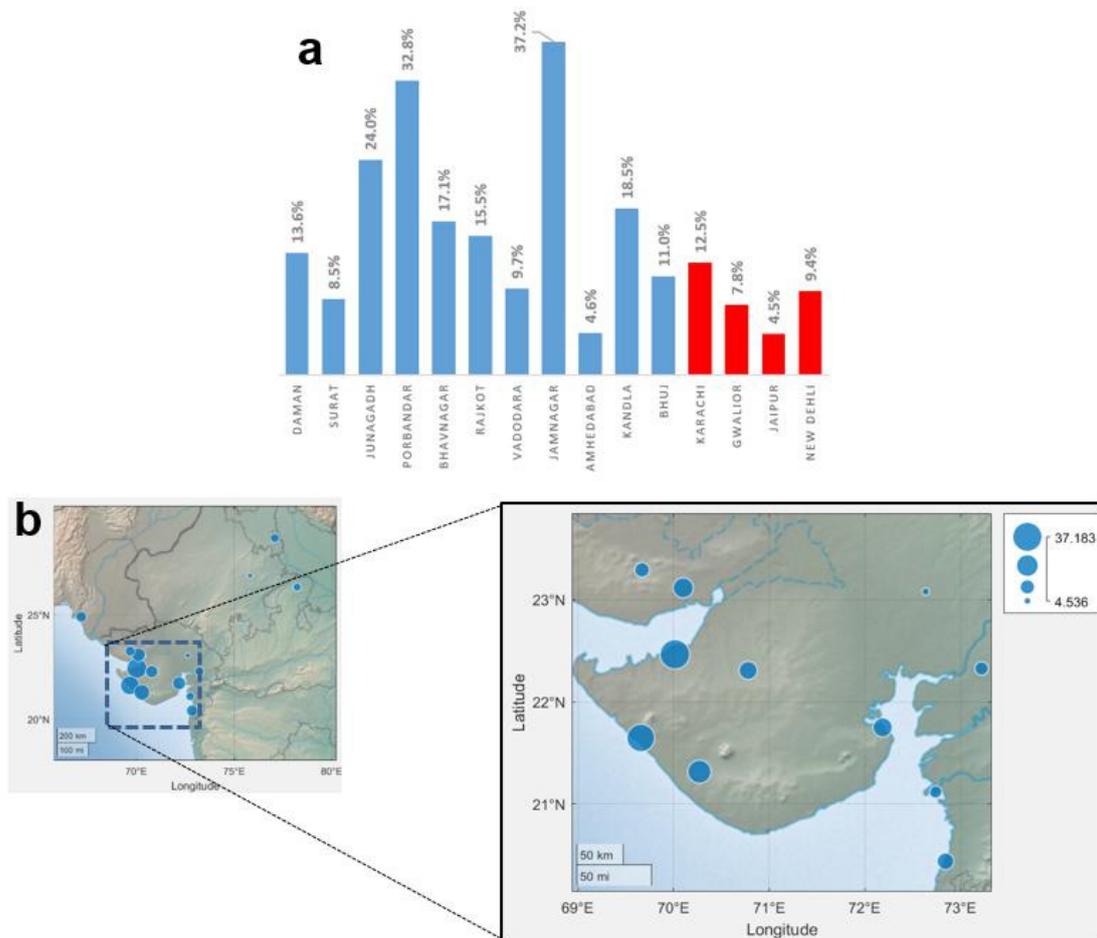
Figure 13. Dew/rain ratio = sum (D) / sum (R) (%) from cumulative yields for dew (sum (D)) and rain (sum (R)) during the dry seasons of the period. (a) Values. Red data are from ERA5 [23] and blue data from the Indian national meteorological network (National Data Centre, Pune). (b) Location of the sites with the dew/rain ratios values.

6. Discussion

6.1. Dew and relative humidity

The general findings of the present study are primarily concerned with the fact that precipitations are weak, unreliable and irregular in months outside the rainy monsoon season. In this time period (October - April), nevertheless, dew occurs very regularity thanks to an efficient radiative cooling in clear and calm nights, as long as the relative humidity of the atmosphere is high enough. As a matter of fact, a close correlation is found between the areas of high relative humidity and the regions of large dew yield (coastal areas of Gujarat, see Fig. 4). This correlation is quite general and is due to the fact that the radiative deficit cannot cool a surface open to air more than a few degrees below the surrounding air temperature. It is within these few degrees cooling that the dew point has to be crossed for condensation to occur, which gives a lower limit for the relative humidity of about 70-80% for dew condensation [3].

6.2. Dew and monsoon

The water resources in India are mostly ruled by the presence of monsoon. Monsoon, indeed, particularly affects India and its surrounding seas. Wind blows from NE during the cooler months of the year and reverses direction to blow from SW during the warmest months. This process brings large rainfalls to the region during June and July and to a lesser extent, August and September.

Monsoon is preceded and followed by a high atmospheric humidity [18]. The presence of relative humidity and then of dew is correlated with the occurrence of the monsoon rains. It results that the future climatic variation of rainfalls should induce the same variation trend for dew. It is also anticipated that the amplitude and evolution of the dew and rain precipitations can be generalized to other places in the world where monsoon is present.

The water resource from dew, although small in amplitude, is nevertheless able to give an important and reliable contribution during the dry season, up to 37% of the rain precipitations (Fig. 14). This is a quite general result, not only observed in the regions of monsoon [15; 31-33], but most generally in other areas of the world during the dry seasons (see e.g. [2, 3]). Dew therefore provides in general a reliable and regular additional moisture resource for plants, and also humans if proper collectors are setup [3].

6.3. Evolution and tendencies for the future years

One of the major results of this study, in addition to assess the important role of dew to give moisture during the dry season, is to detect an increase of dew and rain resources during the 2005-2021 period. This increase contrasts to what is observed in other regions of the world where dew and rain is seen to decrease [3; 9; 34-36], an effect attributed to climate change. As a matter of fact, significant trends were found in calculated dew yields during the time period 1979–2012 [38]. The trends were positive and negative, with values evolving in the range ±15%. In particular, a dew increase was found in the equatorial, monsoon region, in agreement with the present study.

The continuous increase of rainfalls, which is observed during the period 2005-2021, can also be attributed to the climate change [39]. This trend was similarly observed for the seasonal monsoon rain in Southeast Asia, accompanied by an increase of variability of rainfalls [40]. However, it remains very challenging to understand the situation as many parameters are present: Persistence of intense La Nina conditions, abnormal warming of East Indian Ocean, negative Indian Ocean Dipole, southward movement of most of the monsoon depressions and lows and pre-monsoon heating over the Himalayan region that are melting glaciers.

According to the climate scenarios, this trend for rain (increase of variability and amplitude) should then continue in the future years. Due to the increase of relative humidity induced by the monsoon rains enhancement, one expects for dew the same trend (increase) to continue in the future. Further works should precise this point by extracting, as it was done for the Mediterranean basin [4] and north- west Africa [10], the meteo data for years up to 2100 from the low and high emissions representative concentration pathway scenarios (e.g. low global warming RCP 2.6 and high global warming RCP8.5). These data allow dew and rain yields to be estimated with more exactness.

7. Conclusions

The contribution of dew to the water balance was investigated in this work during the dry seasons of the past 17 years between 2005 and 2021. It is seen that dew forms only during the dry season (October to April). By using classical meteorological data, one has determined from an energy-based model the dew potential at 15 airports (14 in India and one in Pakistan). This water resource was mapped over the Gujarat by using a kriging process.

One observes high dew potential with low rain on the coast of the Arabic sea. The situation is inversed for the inland sites, where dew is less but rain is greater. Interestingly, an overall increase in dew water over the whole area is observed during the period, with acceleration after 2015. This increase is, however, heterogeneous. With the exception of the city of Jaipur where the increase is limited to about 2 mm, the areas of New Delhi and Gwalior show a stronger increase in yields (more than 15 mm). According to the site, the dew/rain ratios can represent between 4.6% (Ahmedabad) to 37.2% (Jamnagar) on the whole period of 17 years.

Concerning rain, one observes an increase from SW to NE. The general trend for evolution in the period is the same as dew, with an overall increase, which accelerates after the years 2015-2017. However, while most sites behave as dew, with acceleration after 2015 - 2017, some sites remain stable

(Rajkot, Gwalior). One even notes some sites which undergo a decrease in rainfall from 2015, such as Karachi, Porbandar, Vadodara and Ahmedabad.

It has to be noted that the characteristics of dew and rain are related to the presence of monsoon and thus should be generalized in all areas around the equator where monsoon is present. In particular, the observed increase of dew and precipitations is a rather rare evolution in the context of global warming. This evolution, which is observed since 2015-2017, is likely to continue in the future. The use of climate models should give more information for future trends until the end of the century.

References

1. Mekonnen, M.M., Hoekstra, A.Y. Four billion people facing severe water scarcity. *Science Adv.* **2016**, e1500323.
2. Kuzma, S., Bierkens, M.F.P., Lakshman, S., Luo, T., Saccoccia, L., Sutanudjaja, E.H., Van Beek. R. Aqueduct 4.0: Updated Decision-Relevant Global Water Risk Indicators. *World Resources Institute* **2023**. DOI:https://doi.org/10.46830/writn.23.00061
3. Beysens, D. *Dew water*. River Publishers, Denmark, 2018.
4. Tomaszkiewicz, M. Abou Najma, M., Beysens, D., Alameddine, L., Bou Zeid, E., El-Fadel. M. Projected climate change impacts upon dew yield in the Mediterranean basin. *Sc. Total Environ*. **2016**, 566–567, 1339–1348.
5. Sharan, G., Clus, O., Singh, S., Muselli, M., Beysens, D. Very large dew and rain collector in the Kutch area (Gujarat, India). *J. Hydrol*. **2011a**, 405, 171-181.
6. Sharan, G., Roy, A.K., Royon, L., Mongruel, A., Beysens, D. Dew plant for bottling water. *J. Cleaner Prod*. **2017**, 155, 83-92.
7. Clus, O., Ouazzani, J., Muselli, M., Nikolayev, N., Sharan, S., Beysens, D. Comparison of Various Radiation-cooled Dew Condensers by Computational Fluid Dynamic. *Desalination* **2009**, 249, 707-712.
8. Lekouch, I., Lekouch, K., Muselli, M., Mongruel, A., Kabbachi, B., Beysens, D. Rooftop dew, fog and rain collection in southwest Morocco and predictive dew modeling using neural networks. *J. Hydrol*. **2012**, 448–449, 60-72.
9. Tuure, J., Korpela, A., Hautala, M., Hakojärvi, M., Mikkola, H., Räsänen, M., Duplissy, J., Pellikka, P., Petäjä, T., Kulmala, M., Alakukku, L. Comparison of surface foil materials and dew collectors location in an arid area: A one-year field experiment in Kenya. *Agric. Forest Meteorol*. **2019**, 276, 107613.
10. Muselli, M., Lekouch, I., Beysens, D. Physical and Chemical Characteristics of Dew and Rain in North-West Africa with Focus on Morocco: Mapping Past and Future Evolution (2005–2100). *Atmos*. **2022**, 13, 1974.
11. Raman, C.R.V, Venkataraman, S., Krishnamurthy, V. Dew over India and its contribution to winter-crop water balance. *Agric. Meteo*. **1973**, 11, 17-35.
12. Duvdevani, S. An optical method of dew estimation. *Q. J. R. Meteorol. Soc*. **1947**, 73, 282-286.
13. Sharan, G. Unpublished.
14. Weather and Climate, 2023, https:tcktcktck.org/india/gujarat#::text=Gujarat %20Climate%20Summary,3.98%25%20higher%20than%20India's%20averages. (Accessed on April, 2023).
15. Beysens, D. Estimating dew yield worldwide from a few meteo data. *Atmos. Res*. **2016**, 167,146–155; Beysens, D., 2022. Corrigendum to "Estimating dew yield worldwide from a few meteo data"[Atmospheric Research 167 (2016) 146–155]. *Atmos. Res*. **2022**, 267, 105911.
16. Trosseille, J., Mongruel, A., Royon, L., Beysens, D. Effective surface emissivity during dew water condensation. *Int. J. Heat Mass Transf*. **2022**, 183, 122078.
17. 17. Muselli, M., Clus, O., Ortega, P. Milimouk, I., Beysens, D. Physical, chemical and biological characteristics of dew and rain water during the dry oceans on of tropical islands. *Atmos*. **2020**, 12, 69.
18. Sharan, G., Beysens, D., Milimouk-Melnytchouk, I. A study of dew water yields on Galvanized iron roofs in Kothara (North-West India). *J. Arid Environ*. **2007**, 69, 2, 259-269.

19. Sharan, G., Shah, R., Milimouk-Melnytchouk, I., Beysens, D. Roofs as dew collectors: I. Corrugated galvanized iron roofs in Kothara and Suthari (NW India). In Proceedings of 4th Conf. on Fog, Fog Collect. and Dew 2007 (La Serena, Chile, 23-27 July 2007), p. 301.
20. Sharan, G. Harvesting dew with radiation cooled condensers to supplement drinking water sup- ply in semi-arid. *Int. J. Service Learning in Engineering, Humanitarian Engineering and Social Entrepreneurship* **2011b**, 6, 130-150.
21. Pal Arya, S. Introduction to Micrometeorology. Acad. Press, San Diego, 1988, 307p.
22. Weather Underground database, 2022, https://www.wunderground.com. (Accessed on 13 February 2021).
23. ERA/ECMWS Copernicus database, https://cds.climate.copernicus.eu/cdsapp#!/dataset/reanalysis-era5-single-levels?tab=overview (Accessed on 4 February 2021)
24. NOAA. 2022. Available online: https://www.forecast.weather.gov. (Accessed on 13 February 2021).
25. Beysens, D., Milimouk, I., Nikolayev, V., Muselli, M., Marcillat, J. Using radiative cooling to condense atmospheric vapor: a study to improve water yield. *J.Hydrol*. **2003**, 276, 1-11.
26. Maestre-Valero, J. F., Ragab, R., Martınez-Alvarez, V., Baille, A. Estimation of dew yield from radiative condensers by means of an energy balance model. *J. Hydrol*. **2012**, 460–461, 103–109.
27. Goovaerts, P. Geostatistics for natural resources evaluation. Oxford university press, New York, 1997, 500p.
28. Bargaoui, Z., Chebbi, A. Comparison of two Kriging interpolation methods applied to spatiotem-poral rainfall. *J. Hydrol*. **2009**., 365, 56-73.
29. Lepioufle, J.M., Leblois, E., Creutin, J.D. Variography of rainfall accumulation in presence of advection. *J. Hydrol*. **2012**, 464-465, 494-504.
30. Van de Beek, C.Z., Leijnse, H., Torfs, P.J.J.F., Uijlenhoet, R. Seasonal semi-variance of Dutch rainfall at hourly to daily scales. *Adv. Water Resour*. **2012**, 45, 76-85.
31. Rahmawati, N. Space-time variogram for daily rainfall estimates using rain gauges and satellite data in mountainous tropical Island of Bali, Indonesia (Preliminary Study). *J. Hydrol*. **2020**, 590, 125177.
32. He, S., Richards, K. The role of dew in the monsoon season assessed via stable isotopes in an alpine meadow in Northern Tibet. *Atmos. Res*. **2015**, 151, 101-109.
33. Wenguang, Z., Jingyi, M., Bo, L., Shichun, Z., Jing, Z., Ming, J., Xianguo, L. Sources of monsoon precipitation and dew assessed in a semiarid area via stable isotopes. *Hydrol. Proc*. **2017**, 31,1990-1999.
34. Yang, K., Guyennon, N., Ouyang, L., Tian, L., Tartari, G., Salerno, F. Impact of summer monsoon on the elevation-dependence of meteorological variables in the south of central Himalaya. *Int. J. Clim*. **2018**, 38, 1748-1759.
35. Muselli, M., Beysens, D. Mapping past, present and future dew and rain water resources for biocrust evolution in southern Africa. *J. Hydrol. hydromechanics* **2021,** 69, 400–420.
36. Atashi, N., Rahimi, D., Goortani, B.M., Duplissy, J., Vuollekoski, H., Kulmala, M., Vesala, T., Hussein, T. Spatial and temporal investigation of dew potential based on long-term model simulations in Iran. *Water* **2019**, 11, 2463.
37. Atashi, N., Rahimi, D., Al Kuisi, M., Jiries, A., Vuollekoski, H., Kulmala, M., Vesala, T. and Hussein, T. Modeling long-term temporal variation of dew formation in Jordan and its link to climate change. *Water* **2020**, 12, 2186.
38. 38. Vuollekoski, H., Vogt, M., Sinclair, V.A., Duplissy, J., Järvinen, H., Kyrö, E.M., Makkonen, R., Petäjä, T., Prisle, N.L., Räisänen, P., Sipilä, M. Estimates of global dew collection potential on artificial surfaces. *Hydrol. Earth Syst. Sci*. **2015**, 19, 601-613.
39. Lal, M. Global climate change: India's monsoon and its variability. *J. Environ. Stud. Policy* **2003**, 6, 1-34.
40. Loo, Y.Y., Billa, L., Singh, A. Effect of climate change on seasonal monsoon in Asia and its impact on the variability of monsoon rainfall in Southeast Asia. *Geosci. Front*. **2015**, 6, 817-823.